Ceramics International 30 (2004) 1953–1959

CERAMICS INTERNATIONAL

www.elsevier.com/locate/ceramint

Electrochemical properties of $LiMn_2O_4$ synthesized by the microwave-induced combustion method

Yen-Pei Fu[a,*], Cheng-Hsiung Lin[a], Yu-Hsiu Su[b], Jau-Ho Jean[b], She-Huang Wu[c]

[a] *Department of Chemical Engineering, Wu-Feng Institute of Technology, Ming-Hsiung, Chiayi 621, Taiwan, ROC*
[b] *Department of Materials Science and Engineering, National Tsing-Hua University, Hsinchu 300, Taiwan, ROC*
[c] *Department of Materials Engineering, Ta-Tung University, Taipei 104, Taiwan, ROC*

Received 25 September 2003; received in revised form 13 December 2003; accepted 22 December 2003

Abstract

Spinel $LiMn_2O_4$ powders with small and uniformly sized particle were successfully synthesized by microwave-induced combustion, using lithium nitrate, manganese nitrate, and urea as the staring materials. $LiMn_2O_4$ powders were investigated by X-ray diffractometer (XRD), and scanning electron microscopy (SEM). $LiMn_2O_4$ samples were used as cathode materials for lithium-ion battery, whose discharge capacity and electrochemical characteristic properties in terms of cycle performance were also discussed. The results revealed that the $Li/LiMn_2O_4$ cell synthesized by microwave-induced combustion had a high initial capacity and much better reversibility than one formed in a solid-state reaction.

Keywords: $LiMn_2O_4$ powder; Microwave-induced combustion; Lithium-ion battery; Electrochemical characteristic properties; Cathode

1. Introduction

Spinel-type $LiMn_2O_4$ has recently become an attractive cathode material for making the cathode of lithium ion rechargeable batteries because of its relative low cost and high capacity [1–3]. However, the capacity of $LiMn_2O_4$ fades during cycling for several reasons, such as an instability of an organic-base electrolyte in a high potential region [4], the dissolution of manganese into electrolyte [5,6], change in crystal lattice arrangement with cycling [7], and others. The manganese atom has been partially replaced by transition elements, such as Ni [8,9], Cr [8,9], Co [10], to eliminate capacity fading. The conventional way to produce these materials involved the solid-state reaction of mixing with oxides or carbonates that contain lithium and manganese cations, and calcination at high temperature. However, the solid-state reaction requires a long heating time and followed by several grinding, annealing process, which has some inherent disadvantages, including chemical inhomogeneity, coarser particle size, and introduction of impurities during ball milling.

This work employs a new method called microwave-induced combustion synthesis to produce $LiMn_2O_4$ powders. Microwave processing of materials is fundamentally different from the conventional processing in terms of the heat generation mechanism. In a microwave oven, heat is generated within the sample itself by the interaction of microwaves with the material. Conventional heating generates heat by heating elements and then it is transferred to the surface of sample [11]. The microwave-induced combustion synthesis entails the dissolution of lithium nitrate, manganese nitrate, and urea in water and then heating the resulting solution in a microwave oven. Urea and metal nitrate decompose and giving off flammable gases, such as NH_3, HNCO, O_2, and NO. After the solution reaches the point of spontaneous combustion, it begins to burn in solid form above 1000 °C. The combustion is not complete until all the flammable substances are all burnt out and it turns out to be a loose substance which shows voids, pores, and highly friable formed by the escaping gases during the combustion reaction [12]. The whole process takes only 30 min to yield $LiMn_2O_4$ powders. In this study, spinel $LiMn_2O_4$ powders with uniform, and narrow size distribution are

---

* Corresponding author. Tel.: +886-5-206-3264; fax: +886-5-206-3264.
E-mail address: ypfu@mail.wfc.edu.tw (Y.-P. Fu).

0272-8842/$30.00 © 2004 Elsevier Ltd and Techna Group S.r.l. All rights reserved.
doi:10.1016/j.ceramint.2003.12.183

prepared by microwave-induced combustion and appropriated heating treatment. Moreover, the capacity and reversible performance of the Li/$LiMn_2O_4$ cells are also examined.

2. Experimental procedures

The synthesis process of $LiMn_2O_4$ powders involved the combustion of redox mixtures, in which metal nitrate acted as an oxidizing agent and urea as a reducing agent. The initial composition of the solution containing lithium nitrate, manganese nitrate, and urea was based on the total oxidizing and reducing valences of the oxidizer and fuel using concepts in propellant chemistry [13].

Stoichiometric amounts of lithium nitrate [$LiNO_3$], manganese nitrate [$Mn(NO_3)_2\cdot 6H_2O$], and urea [$CO(NH_2)_2$] were dissolved in 15 ml of water in a crucible. The atomic ratios of Mn/Li were set to be 2. The crucible containing the solution was placed in a microwave oven (CEM, MDS 81D, 650 W). The microwave power of microwave oven operated at 100% (650 W) for 30 min. Initially, the solution boiled and underwent dehydration followed by decomposition with the evolution of large amount of gases (N_2, NH_3, and HNCO). After the solution reached the point of spontaneous combustion, it began to burn with the release of much heat, vaporized all the solution instantly and burnt in solid form above 1000 °C. The entire combustion process for producing $LiMn_2O_4$ powders in the microwave oven took only 30 min, and then the microwave-heated $LiMn_2O_4$ powders were annealed at the temperature range of 600–800 °C for 8 h in air.

Thermogravimetry (TG; Rigaku Thermalplus TG 8120) was used to study the thermal decomposition behavior of the microwave-heated $LiMn_2O_4$ powders. A heating rate of 10 °C/min from room temperature to 900 °C in air. The crystallography of samples were characterized using a computer-interface X-ray powder diffractometer (XRD; Rigaku D/Max-II) with Cu Kα radiation. The lattice constants were calculated against silicon standard (10 wt.%). The total average valences of Mn ion were obtained by potential titration. Firstly, the $LiMn_2O_4$ powders were dissolved in excess of $FeSO_4$ and once the Mn dissolved completely and then the excess $FeSO_4$ was back-titrated with 1N $KMnO_4$ solution. For the total Mn, both Mn^{3+} and Mn^{4+} in the samples were reduced to Mn^{2+} in a mixture solution of HCl and H_2SO_4 under heating. This solution was titrated with 1N $KMnO_4$ around $pH = 7$. $Na_4P_2O_7$ was added to complex the oxidation product Mn^{3+}. The average oxidation state of Mn was calculated by above-mentioned method [14]. The particle morphology and size of the microwave-heated $LiMn_2O_4$ powders and annealed at various temperatures were characterized using a scanning electron microscopy (SEM; JEOL JSM-6500F).

The charge and discharge characteristic of $LiMn_2O_4$ cathode were examined in laboratory cells. The cells consist of a cathode and a lithium metal anode separated by a micro-porous polypropylene separator. The electrolyte used 1 M $LiPF_6$ in a 50/50 vol.% mixture of EC/DMC. The positive electrode was consisted of a mixture of 83 and 10 wt.% of acetylene black, and 7 wt.% polyvinylidene fluoride (PVDF). The mixture was pressed onto a stainless screen mesh at 250 kg/cm^2 and vacuum dried at 110 °C for 12 h in an oven. The cells were cycled in the voltage range of 3.0–4.5 V with typical current density 0.1 mA/cm^2 at room temperature. Cyclic voltammetry was performed for the solid solution using a flooded three-electrode glass cell. The cyclic voltammograms were taken for a sweep rate of 0.05 mV/s between 3.0 and 4.5 V. All assembling of the cell was carried out in a glove box filled with Ar gas.

3. Results and discussion

3.1. Synthesized powders properties

Phase transformation of microwave-heated $LiMn_2O_4$ powders and the mixtures of the reactants $LiCO_3$ with $MnCO_3$ powders were studied using TG measurement. Fig. 1a shows the TG curve for the mixtures of the reactants $LiCO_3$ with $MnCO_3$ powders. There are three steps for the weight loss. The first steps from room temperature to 200 °C may be attributed to the evaporation of residual water; whereas the second step between 250 and 420 °C with sharp weight loss is due to carbon dioxide loss followed by crystallization of $LiMn_2O_4$ phase; the third step appears to be constant for temperature above 450 °C. Fig. 1b shows the TG trace for microwave-heated $LiMn_2O_4$ powders, which indicates the weight loss is about 5% during the whole heating process. This can be attributed to the most $LiMn_2O_4$ spinel phase have been formed during microwave-induced combustion process.

Fig. 2 shows the X-ray diffraction patterns of the microwave-heated $LiMn_2O_4$ powders and the microwave-heated $LiMn_2O_4$ powders annealed at various temperatures. Evidently, the microwave-heated $LiMn_2O_4$ powders contained the spinel $LiMn_2O_4$ phase and Mn_2O_3 phase. The formation of impurity phase (Mn_2O_3) indicated that the temperature is not high enough to reach full crystallization and containing some vacancies in $LiMn_2O_4$ structure during combustion. Therefore, the microwave-heated $LiMn_2O_4$ powders required further thermal treatment. As the microwave-heated $LiMn_2O_4$ powders annealed at 700 °C, the Mn_2O_3 phase disappears and well-crystallized $LiMn_2O_4$ peaks appear with a space group $Fd3m$, where lithium ions occupy the tetrahedral sites (8a), Mn^{3+} and Mn^{4+} ions reside at the octahedral sites (16d), and O^{2-} ions are located at 32e sites [7]. As expected, the crystallization of $LiMn_2O_4$ is further enhanced when the annealing temperature is raised above 700 °C.

Fig. 3 presents the morphology of the microwave-heated $LiMn_2O_4$ powders and the microwave-heated specimens

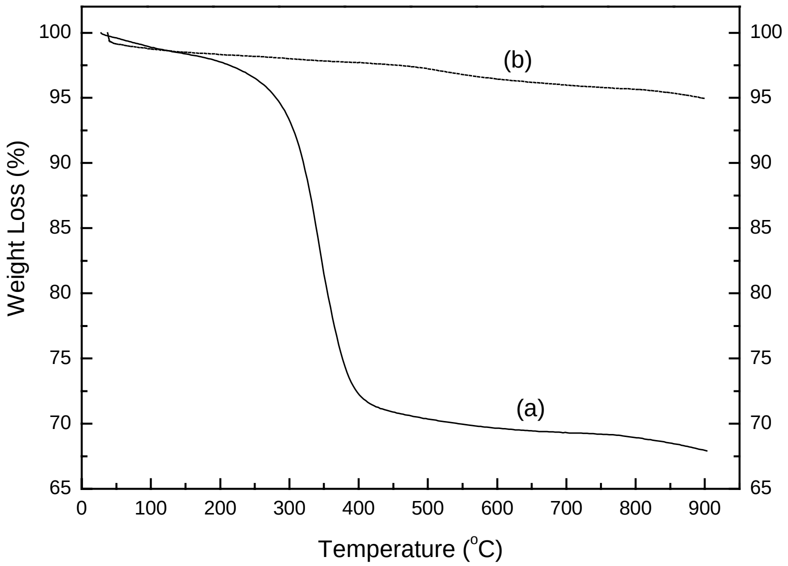

Fig. 1. The thermogravimetric analysis curves for (a) the mixtures of the reactants $LiCO_3$ with $MnCO_3$ powders, (b) the microwave-heated $LiMn_2O_4$ powders.

annealed at various temperatures for 8 h. As shown in Fig. 3a, the microwave-heated $LiMn_2O_4$ powders have nano-sized particle. As shown in Fig. 3b and c, the microwave-heated $LiMn_2O_4$ powders annealed at 600 and 700 °C, respectively, which have broad particle size distribution and form some particle agglomerates. As shown in Fig. 3d, the microwave-heated $LiMn_2O_4$ powders annealed at 800 °C has uniformly sized particles and planar-lamination shape about 0.25 μm in size. According to Fig. 3 results, it is evident that the particle size increases with rising the annealing temperature from 600 to 800 °C.

Heating treatment conditions and the average valence of Mn ion for microwave-heated $LiMn_2O_4$ powders before assembling for cells were presented in Table 1. The variation in lattice parameter and average valence of Mn ion as a function of annealing temperature for $LiMn_2O_4$ powders synthesized by microwave-induced combustion plots in Fig. 4. The average valence of Mn ion decreases from 3.543 to 3.498

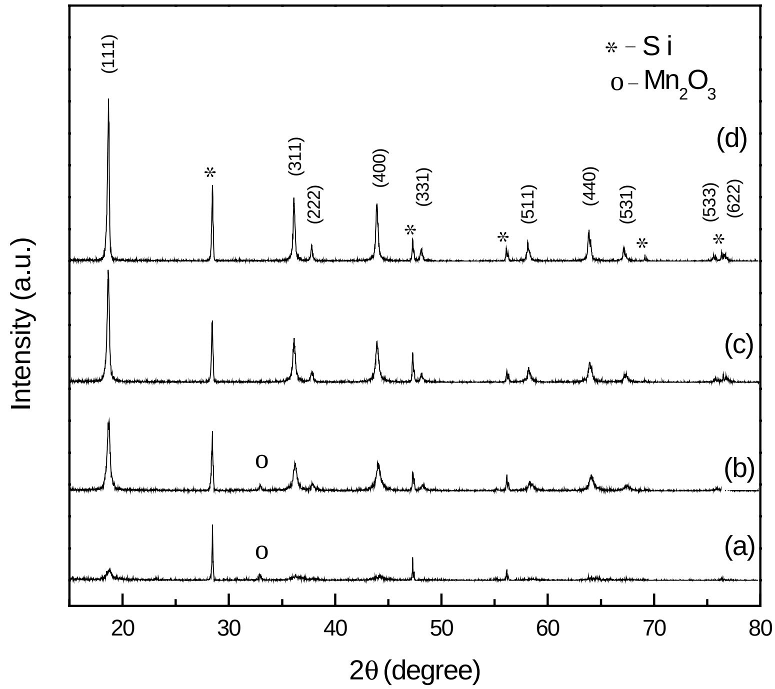

Fig. 2. X-ray diffraction patterns of the microwave-heated $LiMn_2O_4$ powders annealed at various temperatures (a) as-received, (b) annealed at 600 °C for 8 h, (c) annealed at 700 °C for 8 h, (d) annealed at 800 °C for 8 h.

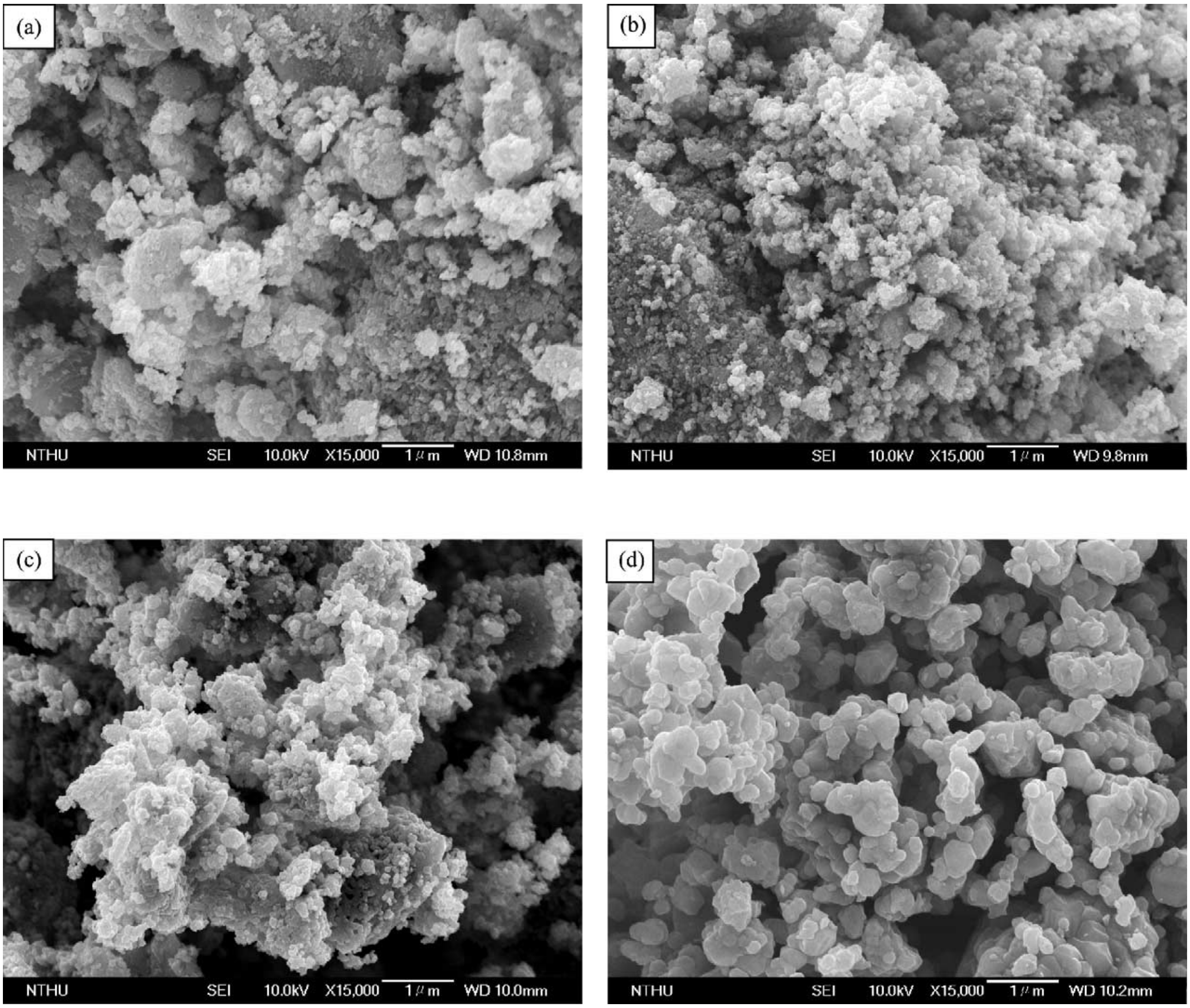

Fig. 3. SEM photographs of the microwave-heated $LiMn_2O_4$ powders: (a) as-received, (b) annealed at 600 °C for 8 h, (c) annealed at 700 °C for 8 h, (d) annealed at 800 °C for 8 h.

as the annealing temperature increases from 600 to 800 °C. This is due to the oxygen loss at high temperature accompanied with the side reaction $Mn^{4+} \rightarrow Mn^{3+}$ [15]. Therefore, a slight higher Mn^{3+} content and lower Mn^{4+} content appears at high annealing temperatures. On the other hand, the lattice constant increases from 8.237 to 8.250 as the annealing temperature increases from 600 to 800 °C. This was due to the larger radius for Mn^{3+} ions (0.72 Å) than Mn^{4+} ion (0.67 Å). Therefore, a high Mn^{3+}/Mn^{4+} ratio is accompanied by high lattice constant at high annealing temperatures.

Table 1
Heating treatment conditions and the average valence of Mn ion for microwave-heated $LiMn_2O_4$ powders before assembling for cells

Sample	Annealing conditions	Mn average valence
A	600 °C for 8 h	3.543
B	700 °C for 8 h	3.510
C	800 °C for 8 h	3.498

3.2. Electrochemical properties

The performance of $LiMn_2O_4$ as the cathode of the lithium-ion battery was examined as follows. Fig. 5 shows the plot of the cyclic voltammogram of $LiMn_2O_4$ cell for the sample A and sample C, with a sweep rate of 0.05 mV/s. The current–voltage curve clearly demonstrated the reversibility of this material upon deintercalation and intercalation of Li^+ over the range of 3.0–4.5 V versus Li/Li^+. Clearly, sample A and sample C both revealed two pairs of redox peaks in cyclic voltammogram, implying lithium ions are extracted and inserted into spinel $LiMn_2O_4$ by a two-step process. For sample A, two anodic peaks were observed at 4.09 and 4.18 V. However, the sample C, yield anodic peaks that are larger and shift toward lower potential, which located at about 4.05 and 4.16 V, respectively.

Fig. 6 shows the plot of the first discharge curves for $Li/LiMn_2O_4$ cells operated between 3.0 and 4.5 V at a constant discharge current density of 01 mA/cm^2. For all samples, two distinct plateaus were observed on the dis-

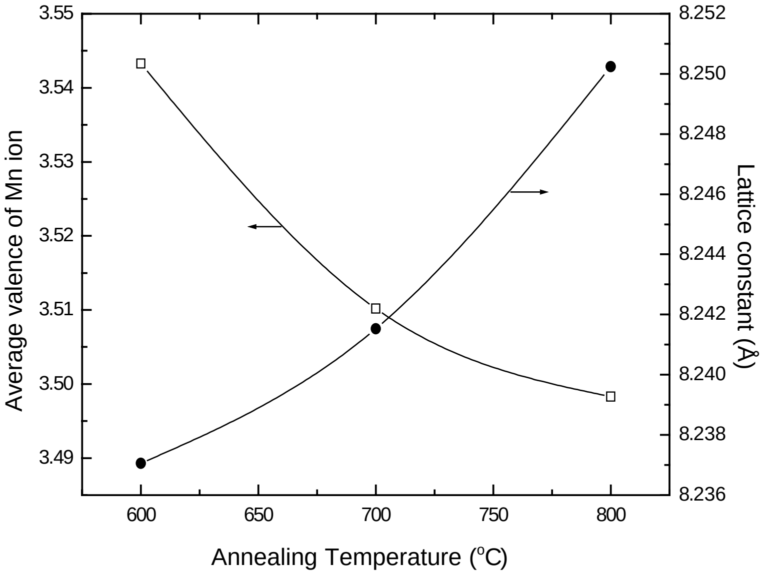

Fig. 4. The lattice parameter and average valence of Mn ion for microwave-heated $LiMn_2O_4$ powders annealing at various temperatures for 8 h.

charge curves. This result is strongly consistent with cyclic voltammogram curve, corresponding to the electrodes undergo two stages of reversible oxidation and reduction process. Moreover, as can be seen in Fig. 5, sample C has much shaper peaks than sample A, indicating flatter discharge curve occurred at sample C. Sample A revealed two plateaus at 4.10 and 3.94 V with the current discharge capacity of 112 mA h/g, compared to sample B had two plateaus at 4.10 and 3.96 V with the current discharge capacity of 125 mA h/g and sample C had two plateaus at 4.10 and 3.97 V with the current discharge capacity of 133 mA h/g at first cycle. Sample A provided a lower initial capacity and not clear plateaus in the discharge curve because of the poor crystallinity of microwave-heated $LiMn_2O_4$ powders annealed at such low temperature (600 °C). Sample C provided the highest initial capacity of 133 mA h/g in the discharge curve for all samples. This value is comparable to the method prepared by solid-state reaction [8] or melt impregnation [16]. Therefore, the $LiMn_2O_4$ powders prepared by microwave-induced combustion method can be used as cathode active materials for lithium-ion battery.

The relationship between the discharge capacity and the cycle number are plotted in Fig. 7 for $Li/LiMn_2O_4$ cells at a current rate of 0.1 mA between 3.0 and 4.5 V with various samples operated at room temperature. The discharge capacity fading of the cells using sample C is a little faster than

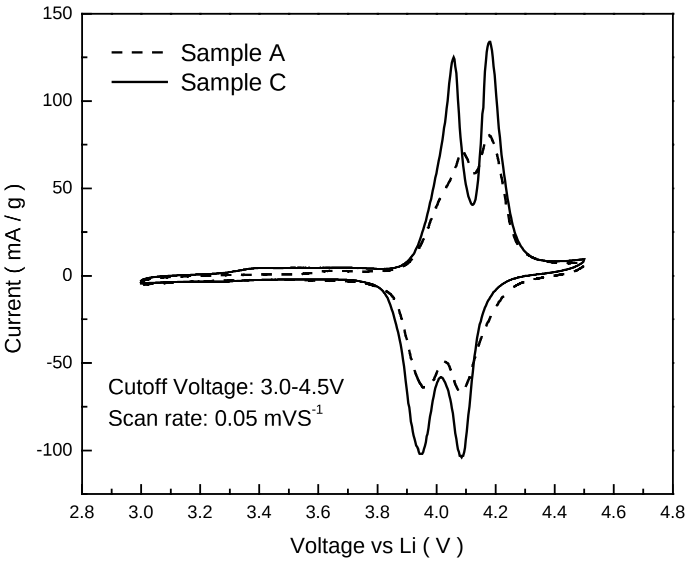

Fig. 5. Cyclic voltammogram over the potential 3.0–4.5 V for sample A and sample C at a scan rate of 0.05 mV/s.

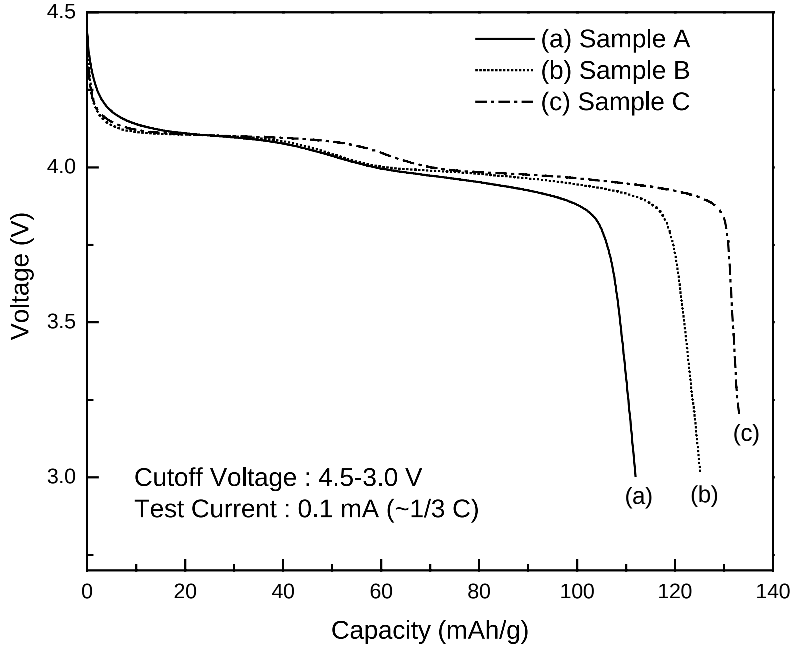

Fig. 6. The first discharge curves for (a) sample A, (b) sample B, and (c) sample C at a current rate of 0.1 mA.

for cells using sample A and sample B. The capacity of loss for the first 20 cycles were about 4.17% of initial capacity for sample A, compared to 7.20 and 8.27% for sample B and sample C. The capacity fading of the cells using solid-state reaction, which was prepared by the mixture of Li_2CO_3 and $MnCO_3$ preheated at 800 °C for 8 h with intermittent grinding and then heated at 800 °C for 24 h in air provided the initial capacity of 118 mA h/g in the discharge curve and the capacity loss about of 4.38% for the first 20 cycles. A comparison of sample C and the solid-state reaction sample reveals that sample C with higher initial capacity but a little faster discharge capacity fading rate for the first 20 cycles, perhaps because of the oxygen loss and higher Mn^{3+} content appeared for the microwave-heated $LiMn_2O_4$ powders annealed at such high temperature (800 °C).

In summary, the $LiMn_2O_4$ powders prepared by microwave-induced combustion processing and appropriated heating treatment with excellent initial capacity and reversible properties compared with solid-state reaction for lithium-ion battery. These results may be due to the $LiMn_2O_4$ powders synthesized by microwave-induced combustion with a higher specific surface area.

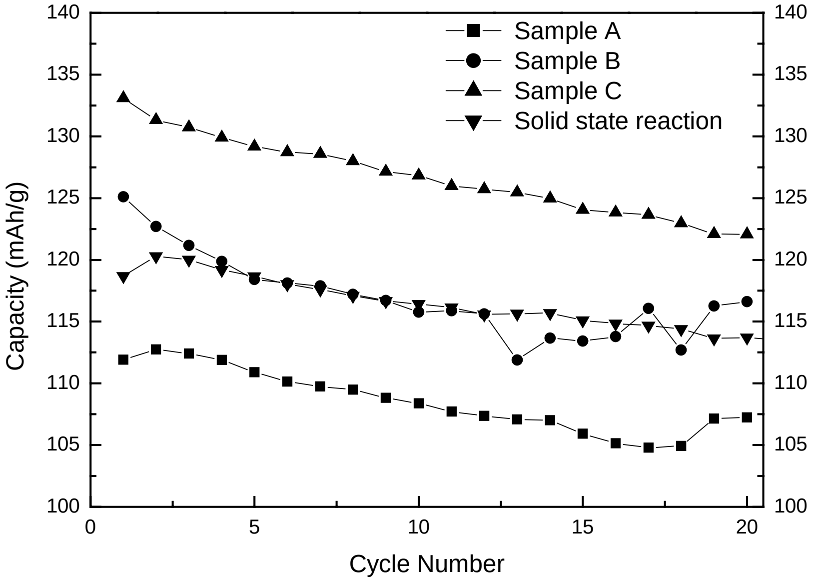

Fig. 7. The variation of discharge capacity as function of cycle number for Li/$LiMn_2O_4$ cells for sample A, sample B, sample C, and the mixture of Li_2CO_3 and $MnCO_3$ powders was preheated at 800 °C for 8 h and finally heated at 800 °C for 24 h in air.

4. Conclusions

Using lithium nitrate, manganese nitrate, and urea as the starting materials, uniform $LiMn_2O_4$ powders have been synthesized successfully by microwave-induced combustion. The results revealed that spinel $LiMn_2O_4$ can be obtained by the microwave-induced combustion in a short time compared with solid-state reaction, moreover the annealing temperature affect greatly the electrochemical properties of $LiMn_2O_4$ samples for lithium-ion battery. Both the initial capacity and magnetization and cycle performance of $Li/LiMn_2O_4$ cell can be significantly improved by appropriate thermal treatment for microwave-heated $LiMn_2O_4$ powders. This method can be employed as a new route for synthesizing analogous materials.

References

[1] S. Komaba, K. Oikawa, S.-T. Myung, N. Kumagai, T. Kamiyana, Solid State Ionics 149 (2002) 47.
[2] D. Song, H. Ikuta, T. Uchida, M. Wakihara, Solid State Ionics 117 (1999) 151.
[3] L. Zhang, H. Noguchi, M. Yoshio, J. Power Sources 110 (2002) 57.
[4] R.J. Gummow, A. de Kock, M. Wakihara, Solid State Ionics 69 (1994) 59.
[5] Y. Xia, Y. Zhou, M. Yoshio, J. Electrochem. Soc. 144 (1997) 2593.
[6] S.-T. Myung, S. Komaba, N. Kumagai, J. Electrochem. Soc. 148 (2001) A482.
[7] P. Arora, B.N. Popov, R.E. White, J. Electrochem. Soc. 145 (1998) 807.
[8] L. Guohua, H. Ikuta, T. Uchida, M. Wakihara, J. Electrochem. Soc. 143 (1996) 178.
[9] K. Amine, H. Tukamoto, H. Yasuda, Y. Fujita, J. Power Sources 68 (1997) 604.
[10] B. Banov, Y. Todorov, A. Trifonova, A. Momchilov, V. Manev, J. Power Sources 68 (1997) 578.
[11] D.E. Clark, W.H. Sutton, Ann. Rev. Mater. Sci. 26 (1996) 299.
[12] O.A. Lopez, J. McKittrick, L.E. Shea, J. Lumin. 71 (1997) 1.
[13] S.R. Jain, K.C. Adiga, V.V.R. Pai, Combust. Flame 40 (1981) 71.
[14] X. Wang, H. Nakamura, M. Yoshio, J. Power Sources 110 (2002) 19.
[15] V. Manev, A. Momchilov, A. Nassalevska, A. Kozawa, J. Power Sources 34 (1991) 147.
[16] M. Yoshio, H. Noguch, H. Nakamura, Y. Xia, H. Takeshige, K. Ikeda, Denki Kagsku 63 (1995) 941.